ISBN: 978-3-95450-249-3 ISSN: 2673-5350 doi: 10.18429/JACoW-IBIC2024-FRBC2

A SYSTEMATIC INVESTIGATION OF BEAM LOSSES AND POSITION RECONSTRUCTION TECHNIQUES MEASURED WITH A NOVEL oBLM AT CLEAR

M. King*,[1], S. Benitez, E. Effinger, J. Esteban, W. Farabolini, J. M. Meyer, B. Salvachua
CERN, Geneva, Switzerland
A. Christie, P. Korysko, Oxford University, Oxford, United Kingdom
C. Welsch, University of Liverpool, Liverpool, United Kingdom
J. Wolfenden, Cockcroft Institute, Daresbury, United Kingdom
[1]also at University of Liverpool, Liverpool, United Kingdom

Abstract

Optical Beam Loss Monitors (oBLMs) allow for cost-efficient and spatially continuous measurements of beam losses at accelerator facilities. A standard oBLM consists of several tens of metres of optical fibre aligned parallel to the beamline, coupled to photosensors at either or both ends. Using the timing information from loss signals, the loss positions can be reconstructed. This contribution presents a novel oBLM system recently deployed at the CERN Linear Electron Accelerator for Research (CLEAR). Multiple methods of extracting timing and position information from measured waveforms are investigated, and the potential impact of varying beam parameters such as bunch charge or number is analysed. This work has resulted in the development of a GUI to aid operations by visualising the beam losses and their positions in real time.

INTRODUCTION

Optical beam loss monitors (oBLM) have become increasingly widespread as distributed beam loss monitoring systems since their first development in 2000 [1]. They consist of a multimode optical fibre with photosensors attached at either or both sides of the fibre. The fibre is placed parallel and as close as possible to the beamline while the photosensors are typically located somewhat shielded from radiation. Whenever beam losses occur, charged particles above a certain threshold velocity traversing the optical fibre induce Cherenkov radiation. A proportion of these photons can be captured by the optical fibre and read out by the photosensors. The signal amplitude then gives the intensity of the beam loss, while the time of arrival of the pulse indicates the loss position.

Previously, multiple studies on oBLMs have been conducted, both at CERN [2, 3], and at other accelerators around the world [4–7]. Depending on the intended use case of the respective installations, fibre thicknesses up to 710 µm and fibre lengths up to 200 m have been studied [5]. In addition, the type and placement of the photosensors vary between different institutes. Although most installations attached Silicon Photomultipliers (SiPMs) to the upstream end of the fibre, some studies chose to instead use Photomultiplier Tubes (PMTs) attached to the downstream end of the fibre [2, 5].

In the following, a novel installation at the CERN Linear Electron Accelerator for Research (CLEAR) will be introduced, and an in-depth investigation of multiple signal analysis and loss position reconstruction techniques discussed.

INSTALLATION

After promising results with a prototype setup at CLEAR [2], it was decided to install a permanent oBLM, covering the entire length of the accelerator. This new setup should help visualise beam losses along the accelerator and thereby help aid with daily beam operations.

CLEAR

CLEAR is a ~40 m long linear electron accelerator at CERN. It consists of a 20 m long accelerating section, split into three structures, followed by a 20 m long experimental beam line. A wide range of parameters can be adjusted with beam energies ranging from 60 MeV to 220 MeV. These beam settings are used to investigate, amongst others, plasma lens and THz acceleration, medical applications of electron beams and various types of beam instrumentation [8, 9].

oBLM

For this installation, it was decided to install a 200 µm thick, 130 m long 'FG200LEA' optical fibre from Thorlabs. This length was needed due to the position of the readout electronics in the gallery above the accelerator. Along the accelerator, optical posts were used to ensure a parallel installation of the fibre at a constant distance of 45 cm to the middle of the beam pipe. This was the closest distance possible due to other beam instrumentation devices along the beam line. The fibre type was chosen as it shows the lowest attenuation overall. As photosensors, S14160-3010PS SiPMs from Hamamatsu were chosen because of their relatively high photon detection efficiency of, at its peak, up to nearly 20 % over a large wavelength range from 300 nm to 900 nm and low operating voltage of 43 V.

LOSS POSITION RECONSTRUCTION

To be able to measure the accuracy of the setup, beam losses were induced at known positions along the beam line.

* m.king@cern.ch

ISBN: 978-3-95450-249-3 ISSN: 2673-5350 doi: 10.18429/JACoW-IBIC2024-FRBC2

At CLEAR, this could be achieved by inserting beam screens in the beam line or by using kicker magnets to divert the beam into the beam pipe. When using kicker magnets, the loss shower is not created at the location of the magnets themselves but approximately 3 m further downstream. The exact location is not only a function of the beam energy and magnet current but also of the exact beam position and angle. Due to this increased uncertainty, it was decided to neglect measurements with losses induced by kicker magnets for the position reconstruction investigations. FLUKA [10–12] simulations indicate that, with the selected configuration, the particle loss shower generates detectable signals from the beam screen location extending up to approximately 2 m away.

In total, four screens along the second part of the beam line were used for this investigation. Losses were created at each of these screens with trains consisting of 5, 10, 30 and 50 bunches to cover a wide range of train charges. The average bunch charge remained consistent at 0.3 nC for all bunch numbers. For each configuration, 20 shots were taken for statistical purposes.

Signal Readout Considerations

Both ends of the fibre are attached to readout boards with SiPMs to save both the up- and downstream waveforms simultaneously. Depending on the use case, using either or both fibre ends may be preferable. From simulations and measurements, the measured signal downstream is greater by nearly one order of magnitude compared to the upstream signal. This can be explained by the loss shower directionality and the limited capture angle of the Cherenkov photons in the fibre.

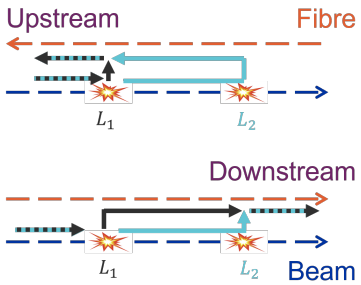

Figure 1: Schematic of two loss positions and the corresponding up- and downstream signal path. In dark blue the direction of the beam, in orange the direction of the photons in the fibre towards the corresponding readout. In black the overall beam and signal path of the loss at L_1, in light blue the same for L_2.

However, it can be easier to resolve signals from different loss locations when using the upstream waveform. This can be best visualised by investigating the signal paths from two loss positions L_1 and L_2 with a certain distance ΔL, as shown in Fig. 1. At the upstream detector, the loss signal from L_2 will arrive slightly after the loss signal from L_1 with the difference in arrival time Δt between these two signals consisting of two parts. The first part corresponds to the time that the beam needs to cover the distance between the two loss locations, i.e. to reach the second loss location. The second part corresponds to the time that the photons need to travel the same distance back. Approximating the speed of the beam with the speed of light in vacuum, c, and the speed of light in the fibre with c/n with a refractive index $n \approx 1.5$, this gives:

$$\Delta t_{\text{Upstream}} = \Delta L\,(1+n)\,/c \approx 2.5\,\Delta L/c.$$

When considering the timing difference for the same two loss positions but for the downstream signal, these two parts are now opposing each other as the overall distance of the beam and signal remains the same. For L_1, the distance ΔL is covered by the photon signal within the fibre travelling at a speed of c/n, for L_2, this distance is covered by the beam at the speed of light. This means that the two parts of the formula above must be subtracted from each other:

$$\Delta t_{\text{Downstream}} = \Delta L\,(1-n)\,/c \approx -0.5\,\Delta L/c.$$

One can now also see that the measured time difference at the downstream sensor contains a scaling factor of ≈ 0.5, i.e. signals will be measured closer in time. This is much lower than the upstream scaling factor of ≈ 2.5. This indicates that from a position resolution point of view, using the upstream signal should be better assuming enough signal can be captured.

The final option is to subtract the time information from the two signals, which eliminates the need for an external trigger. This method also removes the need for a position calibration as the middle of the fibre is exactly when both signals arrive at the same time. In this case, the location along the fibre L is given by:

$$L = \left(t_{\text{Upstream}} - t_{\text{Downstream}}\right)\frac{c}{2n} + \frac{L}{2}.$$

Investigated Conversion Methods

Apart from which fibre end to use, the other main consideration for loss position reconstruction is how to extract a timestamp to convert into a loss position from the measured waveform.

Peak Position Perhaps the most straightforward method is to simply take the time of the maximum of the waveform. However, as this is notably affected by the overall train length, it was decided to subtract half the train length from this time to effectively trigger on the middle of the train and not the start. This was only done for this method as it is most impacted by this effect.

Constant Threshold Another simple method is to apply a constant threshold to all waveforms and then use the first time the signal rises above this level as the loss time. In this case, a value of 15 mV was chosen as the threshold.

ISBN: 978-3-95450-249-3 ISSN: 2673-5350 doi: 10.18429/JACoW-IBIC2024-FRBC2

Constant Fraction Discriminator As a large range of beam train charges are used during day-to-day operations, the loss signal amplitude is expected to vary significantly. One method to minimise the impact of these fluctuations is to use a constant fraction discriminator (CFD). For each waveform, a threshold is set at a fraction of the maximum signal. In this case, after testing multiple values, it was found that a fraction of 40 % is the most consistent.

Gradient The final method investigated was to look at the first-order derivative of the signal. For each waveform, the threshold on the derivative is set to be the maximum of the measured signal divided by 30 ns. Again, multiple values were tested and this value was found to be optimal.

Analysis

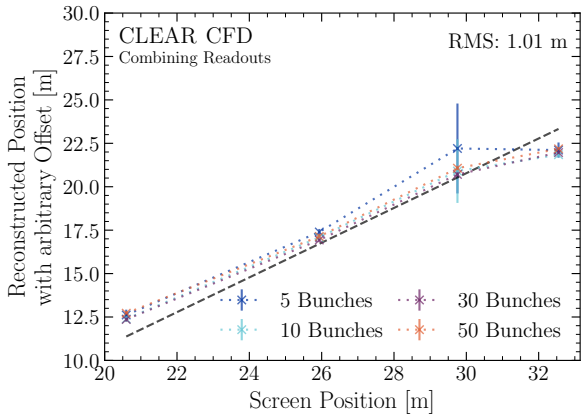

Figure 2: Example plot showing the reconstructed loss position as a function of the screen position for multiple bunch numbers using a constant fraction discrimination and combining readouts. The dashed black line is a fit to this data and the uncertainty on the data points is the standard deviation from the 20 measured waveforms for each point. For all other plots, the reader is referred to the appendix of the presentation. This plot was chosen as it shows the lowest root mean square.

To compare these different methods of signal readout and signal-to-timestamp conversion, the loss waveforms measured at the four screens and for the four different numbers of bunches were converted into positions using all combinations of the readout methods and conversions. This gives sixteen loss position values for each of the twelve possible readout-conversion combinations. These computed positions have a constant offset a compared to the true positions x and therefore a fit of the form $f(x) = x + a$ was performed for all method combinations on all sixteen bunch-screen combinations. As the fibre was installed parallel to the beam line, the slope of this fit function is expected to be exactly one. An example is given in Fig. 2. The fit is shown as the dashed black line and the uncertainties on the data points are the standard deviations calculated from the 20 measured waveforms for each point.

To be able to quantify the accuracy of the readout-conversion combinations, it was decided to calculate the root mean square deviation from the fit. This should give an estimate for the resolution of the method and thereby allow to quantitatively compare all investigated methods.

RESULTS

Table 1: Root Mean Square Deviations From the Fit for All Investigated Readout-Conversion Combinations

	Up	Down	Comb.
Peak Position	1.6 m	3 m	1.59 m
Const. Thresh.	1.45 m	2.7 m	1.33 m
CFD	1.01 m	2.42 m	1.01 m
Gradient	9.63 m	1.99 m	8.12 m

The root mean square deviations from the fit are given in Table 1 with a number of tendencies being clearly visible. Perhaps most strikingly is the accuracy for the downstream readout being roughly a factor two worse than both the upstream readout which itself is slightly worse than the combined readout. From the previously discussed scaling factor of 0.5 compared to 2.5 for the upstream readout and 2 for the combined readout, this effect was expected to be notably more significant. This indicates that the loss resolution is not fully determined by the time resolution of the system but also by fluctuations during the loss shower propagation itself.

Furthermore, the gradient method seems to be the worst by far when considering the upstream and combined readout, despite being the most accurate method for the downstream readout. This can be mainly attributed to the relatively low upstream signal levels of the five bunch measurements. When excluding the five bunch measurements from the calculations, the upstream root mean square deviation is reduced to 0.74 m and the combined readout gives a value of 0.77 m. This is better than all other methods, even when neglecting the five bunch signals for these.

However, when also considering low signals, the best method seems to be using a CFD which is notably better than using a constant threshold which itself is slightly better than using the peak position.

To further increase the achievable loss position resolution, multiple improvements could be made to the overall system and analysis. One could average over multiple waveforms or fit the rising edge to reduce the impact of signal noise. The gain from this is expected to be minimal due to the low statistical uncertainties for most signals and methods. Secondly, increasing the captured signal by using thicker or higher numeric aperture fibres could be of interest.

Finally, and perhaps most importantly, installing the fibre along the beam pipe itself should increase the accuracy of the system. This would reduce shielding and scattering effects from the surrounding instrumentation.

ISBN: 978-3-95450-249-3 ISSN: 2673-5350 doi: 10.18429/JACoW-IBIC2024-FRBC2

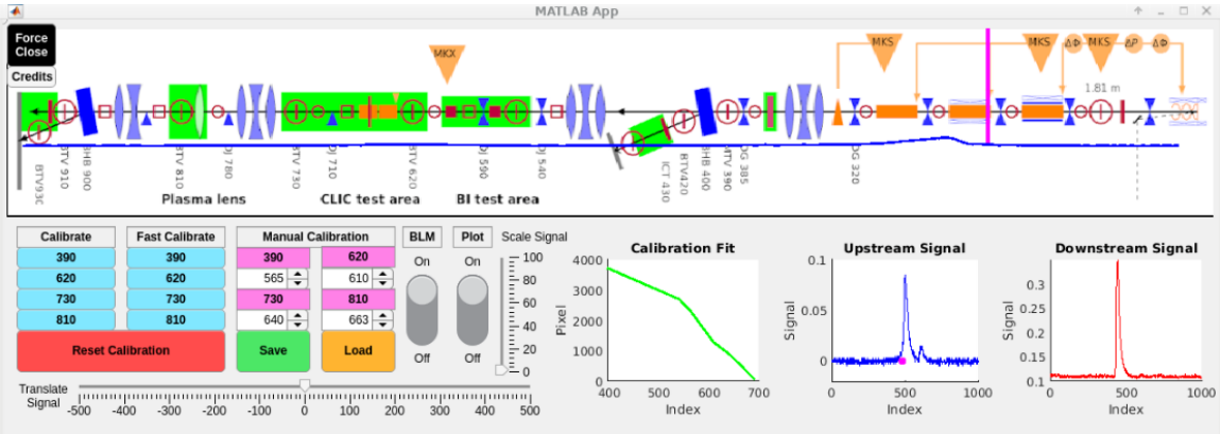

Figure 3: oBLM GUI showing a beam loss occurring at the start (right) of the accelerator, visualised by the pink bar and the blue upstream waveform overlaid on a schematic of the accelerator. Also, various buttons can be seen that can be used to calibrate the loss positions to the known beam screen locations.

However, this is highly difficult, if not impossible, to do at CLEAR, as the fibre would interfere with the need of other experiments to install devices in the beam line.

GUI

These investigations have led to the development of the GUI shown in Fig. 3 which visualises beam loss positions and signals in real time along the entire beam line. The GUI was written in MATLAB and is especially useful when setting up the beam after longer shutdowns or when adjusting beam parameters.

The upper half of the GUI overlays the upstream signal, blue, with a schematic of the accelerator with the beam and the time axis going from right to left. The calculated loss position is given as a pink bar.

On the bottom half of the GUI, buttons representing the screens allow calibration of the setup if necessary. Also, both the upstream and the downstream signal are shown with the later being especially useful for low losses which are not distinguishable from the noise in the upstream signal.

CONCLUSION

The implementation of a permanent oBLM at CLEAR represents a significant advancement in beam monitoring capabilities. Beam loss locations can be measured within an accuracy of 1 m along the entire beam line in real-time. The most accurate method to extract the loss position information has been determined to be using a CFD and combining the waveforms from the upstream and downstream readouts if possible. Overall, this installation has proven to be an invaluable tool for CLEAR beam operations and especially helpful when adjusting beam parameters.

Additional installations at more demanding accelerators around the CERN complex are under development, with further test beam campaigns foreseen to fully explore the potential of oBLMs in the near future.

ACKNOWLEDGEMENTS

The authors thank the entire CLEAR operations team for their help during installation and with the test beam campaign.

REFERENCES

[1] E. Janata and M. Körfer, “Radiation Detection by Cerenkov Emission in Optical Fibers at TTF”, Tesla Report 2000-27, 2000.

[2] S. Benítez Berrocal *et al.*, “Beam Loss Localisation with an Optical Beam Loss Monitor in the CLEAR Facility at CERN”, in *Proc. IPAC’22*, Bangkok, Thailand, Jul. 2022, pp. 351–354. doi:10.18429/JACoW-IPAC2022-MOPOPT045

[3] S. Benítez, B. Salvachúa, and M. Chen, “Beam loss detection based on generation of Cherenkov light in optical fibers in the CERN Linear Electron Accelerator for Research”, *Phys. Rev. Accel. Beams*, vol. 27, no. 5, p. 052901, May 2024. doi:10.1103/PhysRevAccelBeams.27.052901

[4] P. J. Giansiracusa *et al.*, “A distributed beam loss monitor for the Australian Synchrotron”, *Nucl. Instrum. Methods Phys. Res., Sect. A*, vol. 919, pp. 98–104, Mar. 2019. doi:10.1016/J.NIMA.2018.12.054

[5] A. S. Fisher *et al.*, “Beam-Loss Detection for LCLS-II”, in *Proc. IBIC’19*, Malmö, Sweden, Sep. 2019, pp. 229–232. doi:10.18429/JACoW-IBIC2019-TUA002

[6] J. Wolfenden *et al.*, “Cherenkov Radiation in Optical Fibres as a Versatile Machine Protection System in Particle Accelerators”, *Sensors*, vol. 23, no. 4, Feb. 2023. doi:10.3390/s23042248

[7] Y. I. Maltseva and V. G. Prisekin, “Optical Fiber Based Beam Loss Monitor for the BINP e-e+ Injection Complex”, in *Proc. RuPAC’18*, Protvino, Russia, Oct. 2018, pp. 486–488. doi:10.18429/JACoW-RUPAC2018-THPSC38

[8] D. Gamba *et al.*, “The CLEAR user facility at CERN”, *Nucl. Instrum. Methods Phys. Res., Sect. A*, vol. 909, pp. 480–483, Nov. 2018. doi:10.1016/J.NIMA.2017.11.080

ISBN: 978-3-95450-249-3 ISSN: 2673-5350 doi: 10.18429/JACoW-IBIC2024-FRBC2

[9] K. N. Sjobak *et al.*, "Status of the CLEAR Electron Beam User Facility at CERN", in *Proc. IPAC'19*, Melbourne, Australia, May 2019, pp. 983–986. doi:10.18429/JACoW-IPAC2019-MOPTS054

[10] C. Ahdida *et al.*, "New Capabilities of the FLUKA Multi-Purpose Code", *Front. Phys.*, vol. 9, p. 788253, 2022. doi:10.3389/fphy.2021.788253

[11] G. Battistoni *et al.*, "Overview of the FLUKA code", *Ann. Nucl. Energy*, vol. 82, pp. 10–18, 2015. doi:10.1016/j.anucene.2014.11.007

[12] V. Vlachoudis, "FLAIR: A Powerful But User Friendly Graphical Interface For FLUKA", in *Proc. Int. Conf. on Mathematics, Computational Methods & Reactor Physics*, Saratoga Springs, New York, May 2009.